Nondecaying long range effect of surface decoration on the charge state of NV center in diamond

Wei Hu, Zhenyu Li, Jinlong Yang,[a] and Jianguo Hou
Hefei National Laboratory for Physical Sciences at Microscale, University of Science and Technology of China, Hefei, Anhui 230026, People's Republic of China

(Received 10 August 2012; accepted 13 December 2012; published online 15 January 2013)

On the basis of density functional theory, stability and electronic structure of nitrogen-vacancy (NV) centers in surface modified diamond have been studied. Surface decoration is traditionally expected to only have influence on those NV centers close to the surface. However, our calculations indicate that its effect to charged NV centers is nondecaying and long-range, where the formation energy of the charged NV center converges to a value typically different for different types of surface decoration. Such a nondecaying long range effect is due to the electrostatic potential shift induced by the surface dipole layer, and it leads to the preference of NV^- center for oxygen saturated diamond and NV^0 for hydrogenated one. Our work demonstrates that surface functionalization can be used to modify the relative stabilities of differently charged defects in nonmetallic materials. © *2013 American Institute of Physics*. [http://dx.doi.org/10.1063/1.4775364]

Nitrogen-vacancy (NV) centers in diamond have received considerable research interest recently, due to their interesting magnetic and optical properties. Various experimental studies, including electron spin resonance,[1] Rabi oscillations,[2] and single-photon source,[3,4] have been performed on this system. An individual NV center can be used as a qubit, with potential applications in quantum communication[5] and quantum computation.[6,7] Two-qubit operations[8,9] have been demonstrated based on NV centers. Magnetometry[10,11] is also a possible application of NV center.

An NV center is consist of a vacancy with one adjacent carbon atom replaced by a nitrogen atom.[12–14] It mainly has two charge states, the neutral NV^0 and negative NV^-.[15] They can be discriminated by photoluminescence spectroscopy, and it is also possible to interconvert each other via laser excitation.[16] The NV^0 has an unpair electron and is paramagnetic, while NV^- has an $S = 1$ ground state. In high-purity diamond, the NV^- state dominates. Since different charge states lead to different magnetic properties, it is very desirable to control the charge state of NV centers.

Recently, it has been observed that NV^- becomes unstable and tends to be converted into NV^0 close to diamond surfaces[17] and in nanodiamonds.[18] More interestingly, stable NV^- centers can be converted to NV^0 when changing the surface termination from oxygen to hydrogen in single crystal diamond.[19–21] Such a conversion is demonstrated for centers created by ion implantation and annealing in high-purity diamond through selective oxidation.[17] All these experiments demonstrate that surface decoration has an important effect on the relative stabilities of the two NV charge states. Unfortunately, few studies have been focused on the underlying mechanism of the defect stability.[19,21,22]

In the present work, we compare the formation energies of different charge states. Our calculations predict a relative stability change due to different surface functionalizations, which is fully consistent with previous experimental observations. More importantly, we not only show that surface decoration can change chemical environment for those NV centers close to the surface via band bending,[23] but also find that the surface dipole layer induced by polarized chemical bonds on the surfaces has a long range nondecaying impact on the stability of charged NV^- centers. With the increasing of doping depth, the formation energy of a charged NV^- center will converge to a value typically different for different types of surface decorations. Our results provide a facile way to control defect charge states by surface functionalization.

Diamond (100) surface is the most technologically important and the slowest growing surface in chemical-vapor deposition growth of diamond.[24,25] The diamond (111) surface is metallic due to the famous Pandey-chain reconstruction.[26,27] Therefore, it is not conducive to preserve magnetic and fluorescent properties of the NV centers in diamond. Diamond (100) surfaces are considered in this work, including clean (C), hydrogenated (H), ether oxygenated (O), and hydroxylated (OH) surfaces (Figs. 1(a)–1(d)).

The diamond supercell used in this study has a lattice constant of 10.09 Å in both X and Y directions and 40.00 Å in the Z direction with a vacuum layer to form a surface slab model. Both top and bottom surfaces of a slab are decorated by the same functional groups. The slab model for ether oxygenated (100) surface is shown in Fig. 1(c), where there are 15 C–C bond layers in the Z direction. An NV center occupies a C–C bond, with the vacancy closer to the top surface. The NV center doped diamond with different surfaces is denoted as C100_X_i, where X = C, H, O, OH represent different surface functionalization types, and i represents the doping depth measured by the index of corresponding C–C bond layer. It is worth to mention that, if the vacancy were doped in the third

[a]Author to whom correspondence should be addressed. Electronic mail: jlyang@ustc.edu.cn.

 © 2013 American Institute of Physics

Downloaded 15 Jan 2013 to 202.38.88.171. Redistribution subject to AIP license or copyright; see http://jcp.aip.org/about/rights_and_permissions

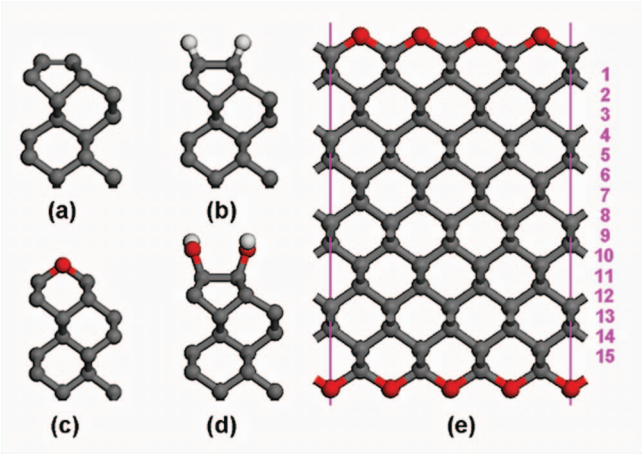

FIG. 1. Atomic structures of (a) clean, (b) hydrogenated, (c) ether oxygenated, and (d) hydroxylated diamond (100) surfaces. (e) Slab model of the ether oxygenated diamond (100) surface. Numbers marked aside are indices of C–C bond layers. White, gray, and red balls denote hydrogen, carbon, and oxygen atoms, respectively.

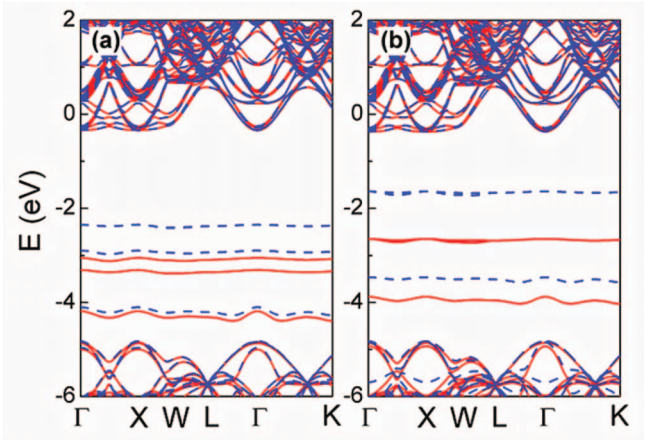

FIG. 2. Electronic band structures for (a) NV^0 and (b) NV^- centers in bulk diamond in the 3 ×3 ×3 supercell. The red solid and blue dotted lines represent spin-up and spin-down states, respectively.

C–C bond layer, the carbon dangling bonds in NV center may be exposed to the air, which would make the NV center unstable and sometimes reconstructed. Therefore, we only consider doping depth larger than 3.

First-principles calculations are based on the density functional theory (DFT) implemented in the SIESTA[28] package. The local spin density approximation[29] is chosen due to its good description of electronic and magnetic properties of the NV centers in diamond on the ground state.[30–32] Test calculations under the generalized gradient approximation of Perdew, Burke, and Ernzerhof[33] give similar results. All the elements (H, C, N, and O) have a double zeta plus polarization orbital basis to describe the valence electrons within the framework of a linear combination of numerical atomic orbitals.[34] The surface Brillouin zone is sampled with a 4 × 4 regular mesh. Atomic coordinates are relaxed using the conjugate gradient algorithm[35] until the energy and force are less than 10^{-4} eV and 0.02 eV/Å, respectively.

As a benchmark, we have calculated the electronic and magnetic properties of NV centers in bulk diamond (3×3 ×3 supercell), which fully agree with previous theoretical calculations.[13,30] Both NV^0 and NV^- centers in diamond are spin-polarized (Fig. 2) with magnetic moments of 1.0 and 2.0 μB, respectively. Three carbon atoms and one nitrogen atom around the vacancy center take a tetrahedral configuration, leading to four states, two fully symmetric a_1 states (one of them lies deep in the valence band of diamond), and two doubly degenerated e_x and e_y states in the NV^- center. These two degenerate states are split in NV^0 due to the Jahn-Teller effect.[31]

In order to evaluate the stability of NV centers doped in diamond with different surfaces, their formation energy[36–39] is defined as

$$E_{form} = E_{doped} - E_{pure} + 2 * \mu_C - \mu_N + q * \mu_e, \quad (1)$$

where E_{pure} and E_{doped} represent the diamond total energy before and after the doping of an NV center with a charge state q, respectively. μ_C and μ_N represent the chemical potential of carbon and nitrogen, which are determined by bulk diamond and nitrogen molecule, respectively. μ_e represents the electron chemical potential of diamond hosting the NV^- centers, which depends on the chemical environment in experiments.[38] In this study, it is aligned with the degenerated NV^- energy level (e_x or e_y) in the spin-up channel, since the NV^- defect is stable when μ_e is above this defect level.[19,21,38]

First, we have checked atomic structures and electronic properties of different diamond surfaces, which are in good agreement with previous theoretical calculations.[40] On the clean diamond (100) surface, two neighboring carbon atoms will form a double-bonded dimer, which introduces occupied π and unoccupied π^* states into the fundamental bandgap of diamond. The hydrogenated diamond (100) surface is the most stable one under normal conditions. Surface hydrogen will remove the π and π^* states, which makes the whole system semiconducting with a wide bandgap. The ether-like configuration is the most stable oxygenated diamond (100) surface, with a C–O–C bridge on the surface. It is semiconducting with a narrow bandgap similar to clean diamond (100) surface. Hydroxylated (100) surface is also semiconducting with a wide bandgap similar to the hydrogenated surface.

When NV centers are formed close to a surface, surface decoration can significantly change their stability. The formation energy strongly depends on the doping depths. We can expect a largely modified formation energy for NV centers close to the surface. And the formation energy is expected to converge to bulk value with the increase of doping depth. This is what we observed for NV^0 centers, as shown in Fig. 3(a). When the doping depth increases to 6, the formation energy is already same for all surfaces and converges to the bulk value (the dashed line in Fig. 3(a)). For a same surface, NV centers prefer to form close to the surface, as also suggested previously.[17,18]

Interestingly, the situation is different for NV^- centers. Although we can still see a convergence of formation energy with doping depth, it converges to different values for different surfaces. Therefore, surface functionalization has a strong effect on stability of NV^- centers. As shown in Fig. 3(b), the

Downloaded 15 Jan 2013 to 202.38.88.171. Redistribution subject to AIP license or copyright; see http://jcp.aip.org/about/rights_and_permissions

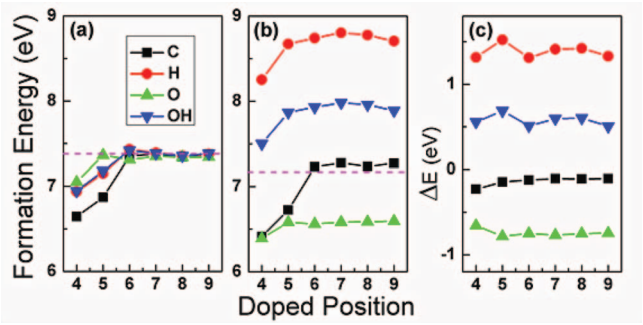

FIG. 3. Formation energy E_{form} for (a) NV^0 and (b) NV^- centers in diamond with clean (C), hydrogenated (H), ether oxygenated (O), and hydroxylated (OH) surfaces. (c) Formation energy difference $\triangle E$ between NV^0 and NV^-. E_{form} of NV centers doped in bulk diamond is marked by horizontal dashed lines.

NV^- center is more stable than NV^0 in bulk, but it is less stable than NV^0 with a hydrogenated surface. This explains previous observed experimental results very well, where the stable NV^- center in diamond trend to turn into NV^0 counterpart when changing the surface termination from oxygen to hydrogen.[19]

When electrons can be freely filled/extracted by, for example, a gate electrode, the ratio of the concentration of NV^- and NV^0 depends on the formation energy difference ($\triangle E$=E_{form}(NV^-)-E_{form}(NV^0)), according to the following relationship:

$$\frac{[NV^-]}{[NV^0]} \propto exp\left(-\frac{\triangle E}{kT}\right), \tag{2}$$

where k is the Boltzmann constant and T is the temperature. In Fig. 3(c), we plot $\triangle E$ versus doping depth. The most important character of $\triangle E$ is that it does not depend on doping depth for a specific surface, which means that the different behavior of NV^- compared to NV^0 is caused by a nondecaying long-range effect. Such an effect is different for different surfaces. The ether oxygenated surface is the most conducive for NV^- formation, followed by the clean surface. On the contrary, the hydrogenated surface is unfavorable to form NV^- centers. Although it is negative for bulk doping, $\triangle E$ already becomes positive with a relatively large absolute value. Therefore, there will be a $[NV^-]/[NV^0]$ ratio inversion as observed experimentally.[19]

We note that the surface which greatly enhances the stability of NV^- is functionalized by electron acceptor groups (oxygen atoms), while the surface which reduces the NV^- stability is a p-type surface covered by hydrogen. Therefore, charge-transfer is expected to make an important role. Chemical interaction between NV center and surface functional groups may affect the defect stability. However, such an interaction is not expected to be long-ranged. In experiment,[41,42] the effect of surface chemical modification on the NV charge state is at least in depth of hundreds of nanometers.

Since diamond is a wide-gap insulator, charge transfer will be localized at surface layer. Therefore, functional groups on diamond surface will induce a surface electric dipole layer.[23,24] As shown in Fig. 4(a), a dipole layer will then generate an electric potential jump

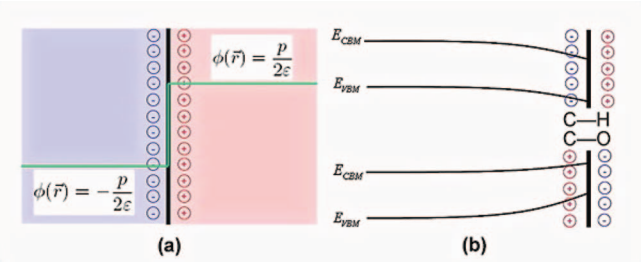

FIG. 4. (a) Electric potential jump produced by a surface electric dipole layer. (b) Band bending close to the surface due to a dipole layer.

$$\phi(\vec{r}) = \frac{\vec{p}}{2\varepsilon} * \frac{\vec{r}}{r}, \tag{3}$$

where $\vec{p}$ and ε represent the electric dipole moment per unit area on the surfaces and the dielectric constant, respectively. Such a constant potential jump will shift the energy bands accordingly, via a band bending close to the surface (Fig. 4(b)). Therefore, a surface dipole layer is ready to provide a long-ranged effect on stability of defects with charges on it. That is why the formation energy of NV^0 converges to the bulk value for all surfaces, while the NV^- formation energy converges to different values for different surfaces. We emphasize that this long-range effect revealed here is intrinsically different from those 1/r decayed Coulomb interaction. Here, the effect in principle does not decay with distance, which provides a versatile means for defect charge state engineering.

A simple model with only the polarized bonds on the surfaces[23] considered can be used to estimate the strength of the surface dipole layer. Based on experimental bond dipole and computationally optimized surface geometry,[43,44] contribution of C^+–$[C{=}C]^-$, C^-–H^+, C^+–O^-, and O^-–H^+ bonds to surface dipole layer is about 1.2, 1.3, 2.5, and 5.0 $\times 10^{-30}$ C · m, respectively. It will then cause a electric potential energy jump of −0.3, 0.4, −0.8, and −0.2 eV, in clean, hydrogenated, ether oxygenated and hydroxylated diamond slab models, respectively. These values are well correlated to the formation energy difference for the NV^- center in diamond.

The mechanism discovered here can be universally applied to a variety of systems with charged defects, for example, color centers in solids.[45] An important system is silicon-vacancy color center in diamond,[12,46] which has a potential to be used as single photon sources. At the same time, this technique can be extended beyond surface chemical modification. Although decorated surface is an ideal model system to study such a long-ranged effect, as a chemical method, it is not very convenient for applications. We emphasize that any method which generates surface electric dipole layer can be used to control the charge state of defects. For example, surface propagating plasmon[47] can be used as a facile way to generate surface dipole layer. Compare to chemical functionalization, a big advantage of using electric method to generate a dipole layer is that it can tune the defect stability reversibly.

We have also checked the band structures of NV centers in diamond with different surface modifications (Fig. 5). Energy shift of diamond-originated bands due to surface modification is clearly seen, consistent with results in formation

Downloaded 15 Jan 2013 to 202.38.88.171. Redistribution subject to AIP license or copyright; see http://jcp.aip.org/about/rights_and_permissions

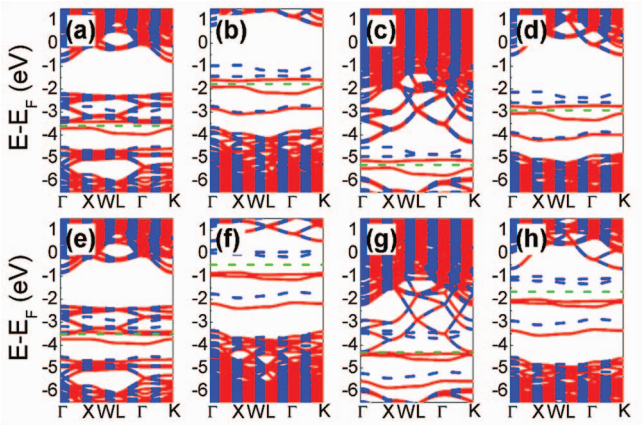

FIG. 5. Electronic band structures for the NV centers in diamond with four different surfaces, NV^0 in (a) C100_C_9, (b) C100_H_9, (c) C100_O_9, (d) C100_OH_9, and NV^- in (e) C100_C_9, (f) C100_H_9, (g) C100_O_9, (h) C100_OH_9. The red solid and blue dotted lines represent spin-up and spin-down states, respectively. The vacuum level is set to zero and the Fermi level is marked by green dotted lines.

energy calculations. For hydrogenated and hydroxylated diamond surfaces, the intrinsic nature of NV centers is well kept, and the defect states shift along with diamond bands. For clean and ether oxygenated surfaces, there are some surface bands in the gap, which overlap with the NV defect states.

In summary, we have investigated the electronic structure of NV centers in diamond affected by chemical surface modifications based on DFT calculations. We find that surface decoration can exhibit long-ranged control of the charge state of NV centers. Different chemical surface modifications strongly affect on the stability of NV^-, but weakly on the NV^0. The formation energy of NV^- can be decreased when electron acceptors exist on the surface, which forms an n-type surface with robust electric dipole layer. The potential jump caused by surface dipole layer is the reason for long-ranged effect on NV^- stability. Results presented here provide a versatile method to control stabilities of charged defect states.

This work is partially supported by the National Key Basic Research Program (2011CB921404), by NSFC (21121003, 91021004, 2123307, 21173202), by CAS (XDB01020300), and by USTCSCC, SC-CAS, Tianjin, and Shanghai Supercomputer Centers.

[1]A. Gruber, A. Dräbenstedt, C. Tietz, L. Fleury, J. Wrachtrup, and C. von Borczyskowski, Science **276**, 2012 (1997).
[2]F. Jelezko, T. Gaebel, I. Popa, A. Gruber, and J. Wrachtrup, Phys. Rev. Lett. **92**, 076401 (2004).
[3]C. Kurtsiefer, S. Mayer, P. Zarda, and H. Weinfurter, Phys. Rev. Lett. **85**, 290 (2000).
[4]A. Beveratos, R. Brouri, T. Gacoin, A. Villing, J.-P. Poizat, and P. Grangier, Phys. Rev. Lett. **89**, 187901 (2002).
[5]L. Childress, J. M. Taylor, A. S. Sørensen, and M. D. Lukin, Phys. Rev. A **72**, 052330 (2005).
[6]A. Nizovtsev, S. Kilin, F. Jelezko, T. Gaebal, I. Popa, A. Gruber, and J. Wrachtrup, Opt. Spectrosc. **99**, 233 (2005).
[7]S. C. Benjamin, D. E. Browne, J. Fitzsimons, and J. J. L. Morton, N. J. Phys. **8**, 141 (2006).
[8]L. Childress, M. V. Gurudev Dutt, J. M. Taylor, A. S. Zibrov, F. Jelezko, J. Wrachtrup, P. R. Hemmer, and M. D. Lukin, Science **314**, 281 (2006).
[9]M. V. G. Dutt, L. Childress, L. Jiang, E. Togan, J. Maze, F. Jelezko, A. S. Zibrov, P. R. Hemmer, and M. D. Lukin, Science **316**, 1312 (2007).
[10]J. R. Maze, P. L. Stanwix, J. S. Hodges, S. Hong, J. M. Taylor, P. Cappallero, L. Jiang, M. V. G. Dutt, E. Dogan, A. S. Zibrov, A. Yacobi, R. L. Walsworth, and M. D. Lukin, Nature (London) **455**, 644 (2008).
[11]G. Balasubramanian, I. Y. Chan, R. Kolesov, M. Al-Hmoud, J. Tisler, C. Shin, C. Kim, A. Wojcik, P. R. Hemmer, A. Krueger, T. Hanke, A. Leitenstorfer, R. Bratschitsch, F. Jelezko, and J. Wrachtrup, Nature (London) **455**, 648 (2008).
[12]J. P. Goss, R. Jones, S. J. Breuer, P. R. Briddon, and S. Öberg, Phys. Rev. Lett. **77**, 3041 (1996).
[13]F. M. Hossain, M. W. Doherty, H. F. Wilson, and L. C. L. Hollenberg, Phys. Rev. Lett. **101**, 226403 (2008).
[14]A. Gali, E. Janzén, P. Déak, G. Kresse, and E. Kaxiras, Phys. Rev. Lett. **103**, 186404 (2009).
[15]L. Rondin, G. Dantelle, A. Slablab, F. Grosshans, F. Treussart, P. Bergonzo, S. Perruchas, T. Gacoin, M. Chaigneau, H.-C. Chang, V. Jacques, and J.-F. Roch, Phys. Rev. B **82**, 115449 (2010).
[16]N. B. Manson and J. P. Harrison, Diamond Relat. Mater. **14**, 1705 (2005).
[17]K. M. C. Fu, C. Santori, P. E. Barclay, and R. G. Beausoleil, Appl. Phys. Lett. **96**, 121907 (2010).
[18]C. Bradac, T. Gaebel, N. Naidoo, J. R. Rabeau, and A. S. Barnard, Nano Lett. **9**, 3555 (2009).
[19]M. V. Hauf, B. Grotz, B. Naydenov, M. Dankerl, S. Pezzagna, J. Meijer, F. Jelezko, J. Wrachtrup, M. Stutzmann, F. Reinhard, and J. A. Garrido, Phys. Rev. B **83**, 081304(R) (2011).
[20]C. Bradac, T. Gaebel, N. Naidoo, M. J. Sellars, J. Twamley, L. J. Brown, A. S. Barnard, T. Plakhotnik, A. V. Zvyagin, and J. R. Rabeau, Nat. Nanotechnol. **5**, 345 (2010).
[21]V. Petráková, A. Taylor, I. Kratochvílová, F. Fendrych, J. Vacík, J. Kučka, J. Štursa, P. Cígler, M. Ledvina, A. Fišerová, P. Kneppo, and M. Nesládek, Adv. Funct. Mater. **22**, 812 (2012).
[22]B. Grotz, M. V. Hauf, M. Dankerl, B. Naydenov, S. Pezzagna, J. Meijer, F. Jelezko, J. Wrachtrup, M. Stutzmann, F. Reinhard, and J. A. Garrido, Nat. Commun. **3**, 729 (2012).
[23]J. B. Cui, J. Ristein, and L. Ley, Phys. Rev. Lett. **81**, 429 (1998).
[24]J. C. Angus and C. C. Hayman, Science **241**, 913 (1988).
[25]C. J. Chu, M. P. D'Evelyn, R. H. Hauge, and J. L. Margrave, J. Appl. Phys. **70**, 1695 (1991).
[26]K. C. Pandey, Phys. Rev. B **25**, R4338 (1982).
[27]S. Iarlori, G. Galli, F. Gygi, M. Parrinello, and E. Tosatti, Phys. Rev. Lett. **69**, 2947 (1992).
[28]P. Ordejón, E. Artacho, and J. M. Soler, Phys. Rev. B **53**, R10441 (1996).
[29]J. P. Perdew and A. Zunger, Phys. Rev. B **23**, 5048 (1981).
[30]A. Gali, M. Fyta, and A. Kaxiras, Phys. Rev. B **77**, 155206 (2008).
[31]A. Gali, Phys. Rev. B **79**, 235210 (2009).
[32]A. Gali, T. Simon, and J. E. Lowther, N. J. Phys. **13**, 025016 (2011).
[33]J. P. Perdew, K. Burke, and M. Ernzerhof, Phys. Rev. Lett. **77**, 3865 (1996).
[34]J. Junquera, Ó. Paz, D. Sánchez-Portal, and E. Artacho, Phys. Rev. B **64**, 235111 (2001).
[35]W. H. Press, B. P. Flannery, S. A. Teukolsky, and W. T. Vetterling, *New Numerical Recipes* (Cambridge University Press, New York, 1986).
[36]C. G. Van de Walle and J. Neugebauer, J. Appl. Phys. **95**, 3851 (2004).
[37]C. W. M. Castleton, A. Höglund, and S. Mirbt, Phys. Rev. B **73**, 035215 (2006).
[38]J. R. Weber, W. F. Koehl, J. B. Varley, A. Janotti, B. B. Buckley, C. G. Van de Walle, and D. D. Awschalom, Proc. Natl. Acad. Sci. U.S.A. **107**, 8513 (2010).
[39]E. M. Benecha and E. B. Lombardi, Phys. Rev. B **84**, 235201 (2011).
[40]S. J. Sque, R. Jones, and P. R. Briddon, Phys. Rev. B **73**, 085313 (2006).
[41]V. Petráková, M. Nesládek, A. Taylor, F. Fendrych, P. Cígler, M. Ledvina, J. Vacík, J. Štursa, and J. Kučka, Phys. Status Solidi A **208**, 2051 (2011).
[42]C. Santori, P. E. Barclay, K.-M. C. Fu, and R. G. Beausoleil, Phys. Rev. B **79**, 125313 (2009).
[43]R. D. Nelson, D. R. Lide, and A. A. Maryott, *Selected Values of Electric Dipole Moments for Molecules in the Gas Phase*, NSRDS-NBS Vol. 10 (U.S. Department of Commerce, Washington, 1967).
[44]K. Dutta, S. K. Sit, and S. Acharyya, Pramana J. Phys. **61**, 759 (2003).
[45]J. H. Schulman and W. D. Compton, *Color Centers in Solids* (Pergamon, New York, 1962).
[46]E. Neu, D. Steinmetz, J. Riedrich-Möller, S. Gsell, M. Fischer, M. Schreck, and C. Becher, N. J. Phys. **13**, 025012 (2011).
[47]A. Huck, S. Kumar, A. Shakoor, and U. L. Andersen, Phys. Rev. Lett. **106**, 096801 (2011).

Downloaded 15 Jan 2013 to 202.38.88.171. Redistribution subject to AIP license or copyright; see http://jcp.aip.org/about/rights_and_permissions